Developmental Biology 373 (2013) 205–215

Contents lists available at SciVerse ScienceDirect

Developmental Biology

journal homepage: www.elsevier.com/locate/developmentalbiology

Evolution of Developmental Control Mechanisms

NF-κB is required for cnidocyte development in the sea anemone *Nematostella vectensis*

Francis S. Wolenski [a], Cynthia A. Bradham [a,b], John R. Finnerty [a,b], Thomas D. Gilmore [a,*]

[a] Boston University, Department of Biology, 5 Cummington Mall, Boston, MA 02215, United States
[b] Program in Bioinformatics, Boston University, Boston, MA 02215, United States

ARTICLE INFO

Article history:
Received 17 May 2012
Received in revised form
12 September 2012
Accepted 4 October 2012
Available online 12 October 2012

Keywords:
NF-kappaB
IkappaB
Nematostella vectensis
Cnidocyte
Development
Evolution

ABSTRACT

The sea anemone *Nematostella vectensis* (Nv) is a leading model organism for the phylum Cnidaria, which includes anemones, corals, jellyfishes and hydras. A defining trait across this phylum is the cnidocyte, an ectodermal cell type with a variety of functions including defense, prey capture and environmental sensing. Herein, we show that the Nv-NF-κB transcription factor and its inhibitor Nv-IκB are expressed in a subset of cnidocytes in the body column of juvenile and adult anemones. The size and distribution of the Nv-NF-κB-positive cnidocytes suggest that they are in a subtype known as basitrichous haplonema cnidocytes. Nv-NF-κB is primarily cytoplasmic in cnidocytes in juvenile and adult animals, but is nuclear when first detected in the 30-h post-fertilization embryo. Morpholino-mediated knockdown of Nv-NF-κB expression results in greatly reduced cnidocyte formation in the 5 day-old animal. Taken together, these results indicate that NF-κB plays a key role in the development of the phylum-specific cnidocyte cell type in *Nematostella*, likely by nuclear Nv-NF-κB-dependent activation of genes required for cnidocyte development.

Introduction

The phylum Cnidaria is an ancient lineage of primarily marine animals comprising over 11,000 species, including sea anemones, corals, hydras and jellyfishes (www.cnidtol.com, Cnidarian Tree of Life; Steele et al., 2011). Cnidarians populate a wide range of marine habitats including coral reefs, estuaries, and even deep water thermal vents. The survival of corals and many sea creatures that live in coral reefs is in peril as environmental changes contribute to the demise of coral reefs around the world (Weis, 2008). Thus, an understanding of the molecular basis of cnidarian physiology and development will be important for assessing environmental effects on cnidarian health.

One phylum-specific cell type that distinguishes Cnidaria from other lineages is the cnidocyte (also known as the nematocyte). There are at least 28 morphologically distinct types of cnidoctye, and they contribute to a range of biological functions including defense, prey capture, environmental sensing and anchoring the animal to its substrate (Kass-Simon and Scappaticci, 2002; Mariscal et al., 1977). The mature cnidocyte contains a collagenous capsule (the cnida or cnidocyst) that is connected to an eversible thread. Many cnidarians have a stinging cell subtype of cnidocyte that discharges venom through a harpoon-like thread in order to capture prey or deter predators (Watson and Mariscal, 1983). Other cnidocytes are thought to be involved in sensing of environmental substances, and may behave somewhat like neuronal sensory cells (Kass-Simon and Scappaticci, 2002). Moreover, treatment of anemones with NANA, an *N*-acetylated sugar derived from mucin, enhances the ability of stinging cnidocytes to fire, supporting the idea that they are regulated by a chemosensory response (Kass-Simon and Scappaticci, 2002; Krayesky et al., 2010; Marlow et al., 2009; Watson et al., 2009).

Nematostella vectensis (Nv) is a small burrowing sea anemone native to estuaries on the Atlantic coast of North America (Reitzel et al., 2008) and is one of the leading model organisms among cnidarians (Darling et al., 2005). In part, this prominence is due to the ease of culturing this small (1–2 cm) anemone in laboratory conditions (Darling et al., 2005), as well as the availability of a complete genome sequence and substantial EST data (Putnam et al., 2007; Sullivan et al., 2006). In *N. vectensis*, cnidocytes are abundant in the tentacles and are also scattered among the ectodermal cells of the external body column and within a limited number of internal sites (Stephenson, 1935). Morphology, size, distribution, and the expression of particular minicollagens (a structural protein in the capsule) have been used to classify *N. vectensis* cnidocytes into three distinct subtypes: basitrichous haplonema, microbasic mastigophores, and spirocysts (Zenkert et al., 2011). While the basitrichous haplonema and spirocyst subtypes are both abundant in the head region, the basitrichous

Abbreviations: Nv, *Nematostella vectensis*; ASW, artificial sea water; BH, basitrichous haplonema; MM, microbasic mastigophore; SC, spirocyst

* Corresponding author. Fax: +1 617 353 6340.
E-mail address: gilmore@bu.edu (T.D. Gilmore).

0012-1606/$ - see front matter © 2012 Elsevier Inc. All rights reserved.
http://dx.doi.org/10.1016/j.ydbio.2012.10.004

haplonema subtype is the dominant cnidocyte in the body column and foot (Zenkert et al., 2011).

NF-κB is an inducible eukaryotic transcription factor that is held inactive in the cytoplasm bound to an inhibitory IκB protein (Hayden and Ghosh, 2004). Activation of cytoplasmic NF-κB generally requires signal-induced degradation of IκB, which enables NF-κB to enter the nucleus where it alters the expression of target genes to bring about cellular and organismal responses. NF-κB can be activated to enter the nucleus in response to a wide range of physiochemical (chemicals, ultraviolet light) and biological (pathogens, cytokines, growth factors, etc.) factors (Gilmore and Wolenski, 2012; Oeckinghaus et al., 2011). NF-κB also plays critical roles in immune system and organ development in a variety of organisms ranging from protostomes to deuterosomes (Hayden and Ghosh, 2004). For example, nuclear localization of the *Drosophila* NF-κB protein Dorsal is necessary to establish dorsal-ventral patterning in the developing fly embryo (Lynch and Roth, 2011). In mammals, NF-κB signaling is also critical for the development of many immune cell types (Gerondakis et al., 2006), the liver (Beg et al., 1995), and the limb bud (Bushdid et al., 1998; Kanegae et al., 1998).

Recently, NF-κB homologs have been identified in a diverse range of simple marine animals (sponges, anemones, and corals) (Gauthier and Degnan, 2008; Shinzato et al., 2011; Sullivan et al., 2007) as well as a unicellular holozoan (Sebé-Pedrós et al., 2011). While several researchers have proposed a role for NF-κB in innate immunity in these basal animals (Augustin et al., 2010; Lange et al., 2011; Meyer et al., 2009; Miller et al., 2007; Shinzato et al., 2011; Sullivan et al., 2007), there is no direct evidence supporting this hypothesis, and the biological function(s) of the NF-κB signaling pathway in these simple marine organisms is unknown.

We previously showed that transcription factor NF-κB is expressed in a subset of ectodermal cells in the body column of *N. vectensis* (Wolenski et al., 2011b). In this report, we show that the majority of the Nv-NF-κB-positive ectodermal cells in juvenile and adult animals are cnidocytes. Moreover, by morpholino-mediated knockdown, we demonstrate that NF-κB is required for cnidocyte development in *N. vectensis*. These results provide the first description of a biological function of NF-κB in an organism basal to arthropods.

Materials and methods

Antisera

Custom antisera were prepared by OpenBiosystems (Fisher Scientific). An affinity-purified rabbit polyclonal antiserum against a C-terminal peptide (PADFLQQGVFSTQNPSNM) of the Nv-NF-κB protein has been described previously (Wolenski et al., 2011b). An affinity-purified guinea pig polyclonal antiserum was prepared against a C-terminal peptide (DNVRPMLQLPESPF) of Nv-IκB. A complete list of antisera, dilutions, and blocking buffers used is provided in Supplemental Table 1.

Plasmid construction, cell culture and transfection

The cDNA encoding Nv-IκB (EU092641.1) was described previously (Wolenski et al., 2011b). Gene-specific primers were used to amplify the Nv-IκB cDNA which was then subcloned into the pcDNA3.1 (+) (Invitrogen) expression vector. Details about the plasmid construction are included in supplemental material.

DF-1 chicken fibroblasts and human A293 cells were grown in Dulbecco's modified Eagle's Medium (Invitrogen) supplemented with 10% fetal bovine serum (Biologos), 50 U/ml penicillin, and 50 μg/ml streptomycin as described previously (Sullivan et al., 2009). Transfection of cells with expression plasmids was performed using polyethylenimine (Polysciences, Inc.) essentially as described previously (Sullivan et al., 2009). Briefly, on the day of transfection, cells were incubated with plasmid DNA and polyethylenimine at a ratio of 1:6. Media was changed 24 h post-transfection, and whole-cell lysates were prepared 24 h later. Alternatively, if cells were used for immunofluorescence, they were passaged onto glass coverslips on the day prior to fixation.

Collection of N. vectensis embryos

The routine maintenance and mating of *N. vectensis* adults were performed as previously described (Fritzenwanker and Technau, 2002; Genikhovich and Technau, 2009; Hand and Uhlinger, 1994). Anemones were raised and spawned in bowls of 1/3 strength artificial seawater (ASW; ~12 parts per thousand). Spawned eggs that were part of an egg mass were de-jellied and collected essentially as described previously (Fritzenwanker and Technau, 2002).

Fixation of anemones

Anemones were prepared for fixation by first placing whole animals in a solution of 7% (w/v) $MgCl_2$ freshly prepared in ASW, and then gently shaking them for 10 min on a rocker as previously described (Wolenski et al., 2011b). After the incubation, anemones were washed 3X with ASW. Anemones were then transferred to 1.5-ml microcentrifuge tubes and fixed in ice cold 4% (v/v) formaldehyde in ASW, with rocking overnight at 4 °C.

Indirect immunofluorescence

Whole-mount indirect immunofluorescence was performed using unfertilized eggs, embryos (0–2 day post-fertilization), juvenile polyps (3–14 days post-fertilization), and small adults (less than 1 cm in size) to determine the expression patterns of Nv-NF-κB and Nv-IκB proteins. Anemones were transferred from the fixative to 12-well plastic dishes and washed 3X with PBT (1X PBS [pH 7.4], 0.2% [v/v] Triton X-100].

Except when anemones were stained with DAPI to detect cnidocytes (see below), antigen retrieval was performed to enhance staining by heating samples in urea (technique modified from Shi et al. (1993)). Briefly, anemones were transferred to glass tubes containing 10 ml of 5% (w/v) urea that had been heated to 80 °C. The tubes were placed in a 1450-watt microwave, heated at the lowest setting for 5 min, and the final temperature of the solution was not allowed to exceed 95 °C. The urea was allowed to cool for 30 min at room temperature, anemones were transferred to a 12-well dish, and washed 4X with PBT. Anemones were incubated overnight in blocking buffer (1X PBT, 5% [v/v] normal goat serum [Gibco], 1% [w/v] bovine serum albumin [Sigma]) at 4 °C.

The next day, the blocking buffer was removed and replaced with primary antiserum (anti-Nv-NF-κB, 1:100; anti-Nv-IκB antiserum, 1:200) diluted in blocking buffer, and samples were incubated with gentle shaking (~80 rpm) for 1.5 h at 37 °C. The primary antiserum was removed and samples were washed 4X with PBT for 10 min each. Secondary antiserum was added and samples were incubated with gentle shaking (~80 rpm) for 1.5 h at 37 °C. In a darkened environment, the samples were washed 4X with PBT for 10 min each. Anemones were then transferred onto a microscope slide and mounted in Vectashield HardSet mounting medium containing DAPI (Vector Labs). Slides were imaged with an Olympus FluoView FV10i confocal microscope. Information on

blocking buffers and antisera dilutions is listed in Supplemental Table 1.

Transfection and indirect immunofluorescence of DF-1 cells were performed essentially as described previously (Wolenski et al., 2011b). Of note, however, when DF-1 cells were probed with anti-Nv-IκB antiserum the blocking buffer was the same as that used for whole-mount staining of anemones (see above).

DAPI staining for cnidocytes

DAPI staining for the poly-γ-glutamate of cnidocytes was performed essentially as described previously (Szczepanek et al., 2002). Anemones were fixed overnight in 4% formaldehyde supplemented with 10 mM EDTA. Samples were then washed three times in Tris-EDTA washing buffer (10 mM Tris, 10 mM EDTA, 10 mM NaCl, pH 7.6), and stained with 140 μM DAPI in Tris-EDTA for 12 min. Anemones were then washed 3X in Tris-EDTA washing buffer and imaged immediately, because the DAPI stain fades within 12 h. Imaging was performed with the Olympus FluoView FV10i confocal microscope using a filter set to a green emission channel (wavelength 521 nm).

When performing a double stain, immunofluorescence was performed first, followed immediately by DAPI staining for cnidocytes. Antigen retrieval was not performed, and all washes, antibody solutions, and mounting media were supplemented to 10 mM EDTA to chelate Ca^{2+}. After the secondary antibody was removed, anemones were washed 1X with PBT, 1X with Tris-EDTA washing buffer, and the DAPI staining was performed as described above. Samples were mounted on microscope slides and imaged immediately.

In situ hybridization

Whole-mount in situ hybridizations were performed according to a previously published protocol (Layden et al., 2010). Briefly, anemones were fixed at either 3 or 21 days post-fertilization. The entire 1423 bp coding region of the Nv-*nfkb* cDNA was subcloned into a pGEM-T Easy (Promega) vector using TA cloning following the manufacturer's instructions. This plasmid contained T7 and SP6 RNA polymerase binding sites that flanked the Nv-*nfkb* gene. An antisense RNA probe was synthesized by in vitro transcription using a Megascript T7 kit (Ambion) and a sense-strand probe was synthesized using a Megascript SP6 kit. Digoxigenin-uridine (DIG-dUTP; Roche Applied Science) was included in the transcription reaction at the ratio of 1:2 to unlabeled dUTP. The RNA probe was diluted in hybridization buffer to a final concentration of 1 ng/μl. Details for the construction of RNA probes are included in the Supplementary information.

Anemones were incubated with the RNA probe at 63 °C for 2 days. The samples were probed with an anti-DIG-dUTP antibody (1:3,000; Roche Applied Science) at 4 °C for 16 h. The anti-DIG-dUTP antibody is conjugated to alkaline phosphatase, which was detected by incubating the anemones in the BM Purple alkaline phosphatase substrate (Roche Applied Science) for 2 h at room temperature. Samples were transferred into 90% glycerol, mounted onto slides, and visualized on a Zeiss AX10 microscope using differential interference contrast (DIC) microscopy.

Preparation of whole-cell lysates and western blotting

Cell lysates were prepared from either human A293 cells or from adult *N. vectensis* using AT lysis buffer as previously described (Wolenski et al., 2011a, 2011b). Although the extraction protocols for both are similar, one difference is that with lysates of A293 cells, the soluble portion of the lysate was analyzed, whereas for extracts from *N. vectensis* the insoluble pellet was analyzed. Western blotting for Nv-IκB was performed essentially as described previously for Nv-NF-κB (Sullivan et al., 2009; Wolenski et al., 2011b), except that the blocking buffer was supplemented with 1% bovine serum albumin. After SDS-PAGE, protein transfer, and probing with guinea pig anti-Nv-IκB primary antiserum, nitrocellulose membranes were incubated with an anti-guinea pig horseradish peroxidase-linked secondary antiserum, and complexes were detected with SuperSignal West Dura Extended Duration Substrate (Pierce).

Morpholino knockdown

Knockdown of the Nv-NF-κB transcript was accomplished by injecting fertilized *N. vectensis* eggs with a transcript-specific morpholino. Injections were performed essentially as described previously (Marlow et al., 2012). The sequences and concentrations of injected morphlinos were as follows: Control, 5′-CCTCTTACCTCAGTTACAATTTATA-3′, 500 μM; Nv-NF-κB, 5′-CCACTTGCTGTTCAGACTGTGTCAT-3′, 500 μM. Morpholinos were co-injected with fluorescein-conjugated dextran. Injected eggs were placed in the dark for 24 h, and then individual embryos were transferred to a single well of a 96-well dish and scored for green fluorescence. Fluorescein emission faded within 48 h, and embryos were fixed five days post-fertilization. Anemones were then co-stained for Nv-NF-κB expression and for the presence of cnidocytes, and animals were scored based on the presence or absence of both stains. The number of DAPI-positive cnidocytes in anemones injected with control or Nv-NF-κB morpholinos was quantified using ImageJ 10.2 according to a previously described method (Burgess et al., 2010).

Results

Nv-NF-κB is expressed in body column cnidocytes

We have previously shown that Nv-NF-κB is expressed in a subset of ectodermal cells, primarily in the lower body column, in both juvenile (polyp) and adult anemones (Wolenski et al., 2011b). We hypothesized that the Nv-NF-κB-positive cells were cnidocytes (Wolenski et al., 2011b), based on their elongated cell shape and because some cnidocytes have been reported to show a pattern of staining similar to Nv-NF-κB (Marlow et al., 2009, 2012; Szczepanek et al., 2002). Therefore, we used fixation and staining methods that would enable us to determine whether Nv-NF-κB-positive cells also stained positive for a cnidocyte marker. Under Ca^{2+}-free conditions cnidocytes can be stained with DAPI, which binds to abundant poly-γ-glutamate in the cnidocyte capsule only in the absence of Ca^{2+} (Szczepanek et al., 2002). Although DAPI is typically used as a DNA stain that fluoresces in a blue channel, the emission spectrum shifts to green when DAPI is bound to poly-γ-glutamate, permitting the discrimination of cnidocyte- and DNA-specific labeling (Szczepanek et al., 2002).

Juvenile anemones (polyps) were co-stained for Nv-NF-κB and for cnidocytes. Anti-Nv-NF-κB-positive cells were detected with a Texas Red-conjugated secondary antiserum; of note, signal was detected in the red, but not green, fluorescence channel (Fig. 1A, right). In contrast, cnidocyte staining with DAPI was detected in the green fluorescence channel (Fig. 1B, left), but not in the red channel (Fig. 1B, right). The Nv-NF-κB fluorescence was detected in a subset of body column cells (Fig. 1C, left), whereas mature cnidocytes were detected in both the body column and tentacles of the anemone (Fig. 1C, middle). Merging of the images of anti-Nv-NF-κB and DAPI staining revealed that most Nv-NF-κB-positive cells were also DAPI-stained cnidocytes located in the body column (Fig. 1C, right). At higher magnification, Nv-NF-κB appeared to be localized in the cytoplasm of these cells, which

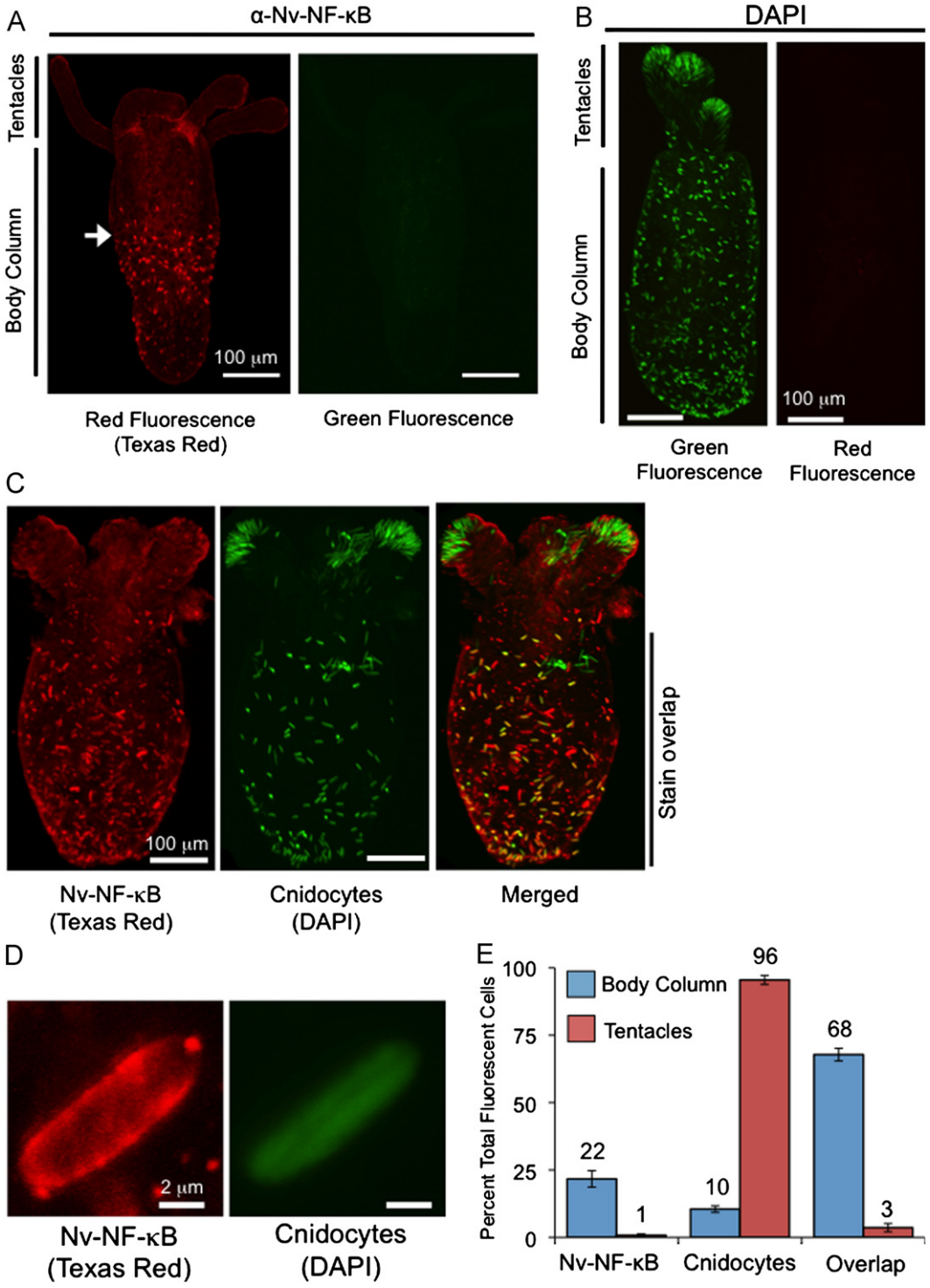

Fig. 1. Nv-NF-κB is expressed in a subset of cnidocytes in *N. vectensis*. (A) Whole-mount immunofluorescence was performed on polyps with anti-Nv-NF-κB antiserum, detected with Texas Red-conjugated secondary antiserum, and visualized in red (left) and green (right) fluorescence channels. The white arrow indicates specific fluorescence. (B) Anemones were fixed and stained under calcium-free conditions. DAPI staining of a juvenile polyp was imaged to detect green (left) and red (right) fluorescence. (C) Whole-mount immunofluorescence was performed with anti-Nv-NF-κB antiserum. Nv-NF-κB (Texas Red, left panel) was detected in body column cells but not in the tentacles. DAPI (middle panel) stained all cnidocytes. An overlapped image shows Nv-NF-κB expression in many body column cnidocytes (right panel). (D) Higher magnification of a single cnidocyte that stains positive for Nv-NF-κB (left). The internal capsule is stained with DAPI (right). The tentacles and body column are indicated by black bars. White bars indicate scale. (E) A total of 1,036 fluorescent cells in the body column and 579 from the tentacles were counted in five anemones. These were sorted based on staining for Texas Red (Nv-NF-κB), DAPI (cnidocytes) or both. Values are given as percentages of total fluorescent cells in either the body column (blue bars) or the tentacles (red bars). Error bars indicate Standard error. (For interpretation of the references to color in this figure legend, the reader is referred to the web version of this article.)

surrounds the mature cnidocyte capsule (Fig. 1D). Quantification of co-stains for Nv-NF-κB and DAPI in the body column showed that 68% of the DAPI-stained cnidocytes were also positive for Nv-NF-κB (Fig. 1E; right column, blue bar). In the tentacles only 3% of the DAPI-positive cnidocytes also stained positive for Nv-NF-κB (Fig. 1E; right column, red bar).

N. vectensis has three subtypes of cnidocytes that can distinguished by size: basitrichous haplonema (BH) cnidocytes are approximately 12 μm; microbasic mastigophores (MM) are 17–20 μm; and spirocysts (SC) are 25–30 μm (Zenkert et al., 2011). In addition, these cnidocyte subtypes are not evenly distributed across the animal; in particular, the BH subtype comprises 80–90% of cnidocytes in planula larvae and juvenile polyps and in the body columns of adult polyps, whereas the SC subtype is prevalent only in tentacles, and the MM subtype comprises 10–20% of cnidocytes in both the tentacles and body column. The average length of Nv-NF-κB-positive cnidocytes was determined to be 11.1 μm +/−0.2 μm (Supplemental Table 2). Thus, the distribution and size of Nv-NF-κB-positive cnidocytes indicate that they are part of the BH subtype of cnidocytes.

To address the possibility that the staining of cnidocytes with our Nv-NF-κB antiserum was an artifact of, for example, non-specific binding of primary or secondary antiserum to these unusual cells, we performed two experiments. First, we performed in situ hybridization using an anti-sense RNA probe for Nv-*nfkb*. The hybridized anti-sense probe was then detected using an alkaline phosphatase-based colorimetric assay. Staining for Nv-*nfkb* was observed in elongated ectodermal cells in 3-d post-fertilization embryos (Fig. 2, left panel), and staining of a 21-d post-fertilization animal is located primarily in the ectoderm of the lower body column (Fig. 2, right panel). Other anemones at the same stages showed similar staining, and no specific staining was seen with a sense-strand Nv-*nfkb* probe (Supplemental Fig. 1). Thus, the Nv-*nfkb* transcript is expressed in a general pattern that is similar to the staining seen with the anti-Nv-NF-κB antiserum. Second, we performed indirect immunofluorescence on whole-mount polyps using a distinct primary rabbit antiserum, namely one that recognizes the serontonin receptor 5HT, which has also previously been shown to stain scattered ectodermal cells in the body column of *Nematostella* (Marlow et al., 2009, 2012). The staining for 5HT was clearly distinct from the staining seen with the anti-Nv-NF-κB antiserum: (1) the morphologies of the 5HT-positive and Nv-NF-κB-positive cells are clearly distinct (round vs. elongated, respectively), and (2) the two cell types could easily be distinguished when co-staining was performed using both primary antisera and a single anti-rabbit secondary antiserum (Supplemental Fig. 2). Thus, different primary rabbit antisera that were simultaneously probed with the same secondary antiserum detected distinct subsets of ectodermal cells. Moreover, we have previously shown that no staining of ectodermal cells is seen using a pre-immune rabbit serum (Wolenski et al., 2011b). Taken together, the results in this section provide strong evidence that the cnidocyte-specific staining seen with the anti-Nv-NF-κB antiserum is genuinely detecting expression of Nv-NF-κB in animals.

Nv-NF-κB expression is first detected at 30 h post-fertilization in developing embryos

The NF-κB pathway plays critical roles in the development of tissue subtypes in many animals ranging from *Drosophila* to vertebrates (Beg et al., 1995; Bushdid et al., 1998; Gerondakis et al., 2006; Hayden and Ghosh, 2008; Kanegae et al., 1998; Lynch and Roth, 2011). Therefore, we next determined when and where Nv-NF-κB was expressed during embryonic development.

To characterize the developmental expression of Nv-NF-κB, freshly laid eggs were fertilized, and embryos were collected at different time points and subjected to indirect immunofluorescence with anti-Nv-NF-κB antiserum. Nv-NF-κB was not expressed in unfertilized eggs or embryos up to 24 h post-fertilization (Fig. 3A–D). Nv-NF-κB was first detected in a few scattered embryonic cells at 30 h post-fertilization (Fig. 3E). Cnidocyte-shaped cells were first detected at 40 h post-fertilization and were prevalent throughout animals at later stages of development (Fig. 3F and G). Of note, the staining of Nv-NF-κB shown in Fig. 3 required treatment with urea (i.e., antigen retrieval for enhanced staining, see Materials and Methods), which prevented the use of DAPI for staining of cnidocyte capsules. Nevertheless, the results in this section establish that Nv-NF-κB is first expressed approximately 30 h post-fertilization, a timing that is similar to the reported appearance of cnidocytes at 24–48 h post-fertilization (Marlow et al., 2009).

Nv-NF-κB is localized in the nucleus of 30-h post-fertilization embryos

The subcellular localization of Nv-NF-κB in embryonic cells was also determined. High resolution optical sections of the ectoderm in 30-h post-fertilization embryos were imaged with confocal microscopy. In these cross sections, Nv-NF-κB was detected in the nuclei of cells at 30 h post-fertilization (Fig. 4A, arrows).

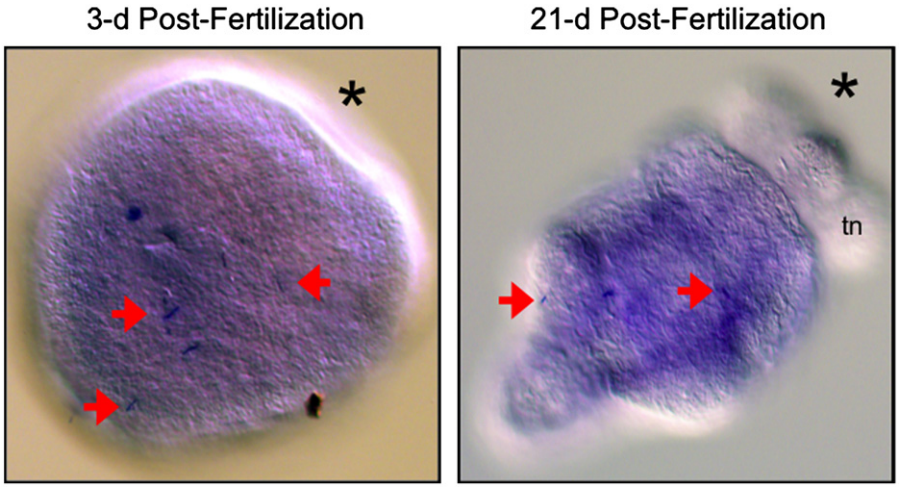

Fig. 2. Nv-*nfkb* mRNA is expressed in scattered cells in the ectoderm of *N. vectensis*. An in situ hybridization was performed using anti-sense RNA that had been transcribed from Nv-*nfkb* cDNA. The RNA probe contained DIG-dUTP nucleotides, which were detected by an anti-DIG antibody that was conjugated to alkaline phosphatase. Phosphatase activity was visualized by cleavage of the substrate BM Purple. Staining of a 3-d post-fertilization embryo (left panel). Staining of a 21-d post-fertilization polyp (right panel). Specific staining of individual ectodermal cells is indicated by red arrows. The oral end of each animal is indicated by an asterisk, and tentacle buds in the 21-d anemone (tn) are as indicated. All images were taken with a Zeiss AX10 microscope under DIC light. (For interpretation of the references to color in this figure legend, the reader is referred to the web version of this article.)

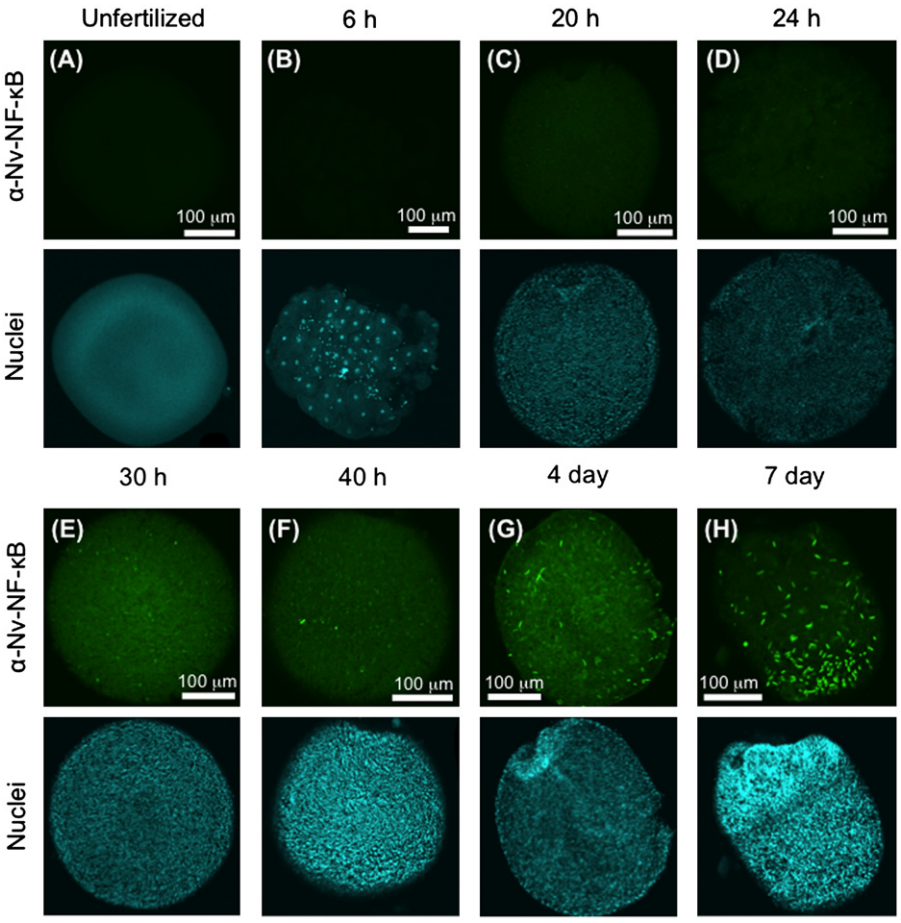

Fig. 3. Nv-NF-κB expression in developing *N. vectensis* embryos. Eggs and embryos were taken from a single spawning event. (A)–(H) Whole-mount immunofluorescence was performed with anti-Nv-NF-κB antiserum and antigen retrieval was performed with urea to enhance staining. Nv-NF-κB (top panels) was detected with FITC-conjugated secondary antiserum and nuclei were detected with DAPI (lower panels). Embryos were fixed at various time points ranging from unfertilized eggs (A) to hours (B)–(F) and days (G) and (H) post-fertilization. All images were taken using a FluoView FV10i confocal microscope with the same settings for FITC (green) detection. White bars indicate scale. (For interpretation of the references to color in this figure legend, the reader is referred to the web version of this article.)

At increased magnification, individual nuclei clearly stained positive for both Nv-NF-κB and DAPI, under normal conditions in which nuclei stained with DAPI are detected in the blue channel (Fig. 4A; inset, arrows; Supplemental Fig. 3).

The distribution of Nv-NF-κB-positive cells was clearly limited to the ectoderm in the 3-day post-fertilization embryo (Figs. 4B and C). In a focal plane taken through the embryo, the ectoderm appears as a single layer of cells that surrounds the endoderm (Fig. 4B, ectoderm demarcated by white arrows). At higher magnification, Nv-NF-κB was detected in the cytoplasm of these ectodermal cells (Fig. 4C, red arrows). The cytoplasmic subcellular localization of Nv-NF-κB at this stage is consistent with that seen in 4 week-old polyps and adults (Wolenski et al., 2011b).

Morpholino-based knockdown of Nv-NF-κB abolishes cnidocyte development

To determine whether Nv-NF-κB expression is required for cnidocyte development, fertilized eggs were microinjected with a morpholino-substituted antisense oligonucleotide (MO) specific for Nv-NF-κB, and the expression of Nv-NF-κB and the appearance of cnidocytes were assessed five days later. Microinjection of a control MO did not appear to affect the development of Nv-NF-κB-positive cnidocytes (Fig. 5, top). In contrast, microinjection of the Nv-NF-κB MO abolished expression of Nv-NF-κB in 5-day post-fertilization animals, and approximately 90% (60 of 66) of 5-day animals that developed from fertilized eggs micoinjected with Nv-NF-κB MO did not stain positive (by DAPI) for cnidocytes (Fig. 5, bottom). The average number of Nv-NF-κB-positive cells, as determined by analyzing optical cross sections of MO-injected anemones, was much lower for anemones injected with the Nv-NF-κB MO (1 positive cell/anemone) than for those injected with the control MO (135 positive cells/anemone) (Supplemental Table 3).

Nv-IκB is expressed in Nv-NF-κB-positive ectodermal cells in juvenile and adult N. vectensis

We have previously shown that Nv-IκB can directly bind and inhibit Nv-NF-κB (Wolenski et al., 2011b). Using a newly generated anti-Nv-IκB antiserum, we next sought to determine the expression pattern of Nv-IκB. To demonstrate the specificity of the antiserum, we first used Western blotting to show that the Nv-IκB antiserum detected a single, specific band in lysates of A293 cells transfected with an Nv-IκB expression plasmid and in extracts from anemones, whereas blotting with a pre-immune serum did not detect the anti-Nv-IκB-reactive band (Fig. 6A). In addition, the anti-Nv-IκB antiserum readily detected over-expressed Nv-IκB in the cytoplasm of DF-1 chicken fibroblasts transfected with a pcDNA-Nv-IκB expression vector (Fig. 6B, right), whereas no staining was seen with pre-immune serum (Fig. 6B, left). The cytoplasmic localization of Nv-IκB in DF-1 cells is consistent with our previously published data using a Myc-tagged Nv-IκB protein (Wolenski et al., 2011b).

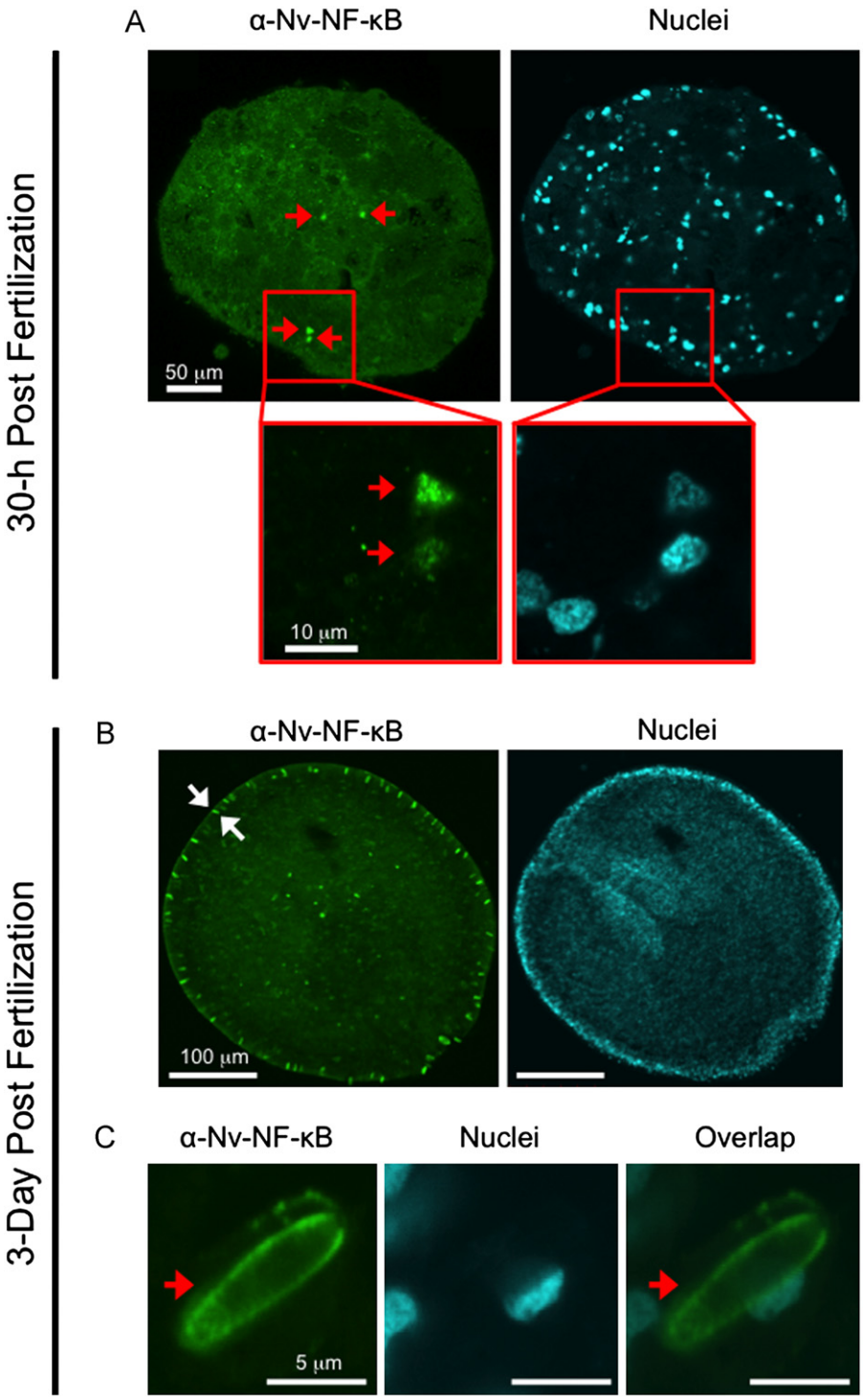

Fig. 4. Nv-NF-κB is localized in the nucleus of cells in 30-h post fertilization *Nematostella* embryos. (A)–(C) Whole-mount immunofluorescence was performed with anti-Nv-NF-κB antiserum and antigen retrieval was performed with urea. (A) Nv-NF-κB (left panels) was detected with FITC-conjugated secondary antiserum and nuclei were detected with DAPI (right panels). The inserts show a higher magnification of a region containing nuclear Nv-NF-κB staining. All images are cross-sections of the ectoderm imaged with a FluoView FV10i confocal microscope. Red arrows indicate overlapping staining for Nv-NF-κB (FITC) and nuclei (DAPI). (B) A confocal cross-section showing staining of a 3-day post-fertilization embryo. The ectoderm is demarcated as the area between the two white arrows and forms a ring around the endoderm. (C) Higher magnification of a single cnidocyte (red arrows) that stains positive for Nv-NF-κB (left). The nucleus of the cell is located immediately under the FITC-stained cytoplasm. White bars indicate scale. (For interpretation of the references to color in this figure legend, the reader is referred to the web version of this article.)

To identify cells in *N. vectensis* that express Nv-IκB, indirect immunofluorescence was performed with the anti-Nv-IκB antiserum, which was then detected with FITC-conjugated secondary antiserum. In whole-mount staining of polyps, no signal was detected with pre-immune serum (Fig. 6C, left), but numerous positive ectodermal cells were detected with the anti-Nv-IκB antiserum (Fig. 6C, right). The subcellular localization of Nv-IκB in whole-mount anemone preparations was difficult to ascertain, but it did not appear to be strictly limited to the cytoplasm or nuclei of cells.

The anti-Nv-IκB staining of a subset of cells in the body column ectoderm of juvenile and adult anemones is similar to that seen with

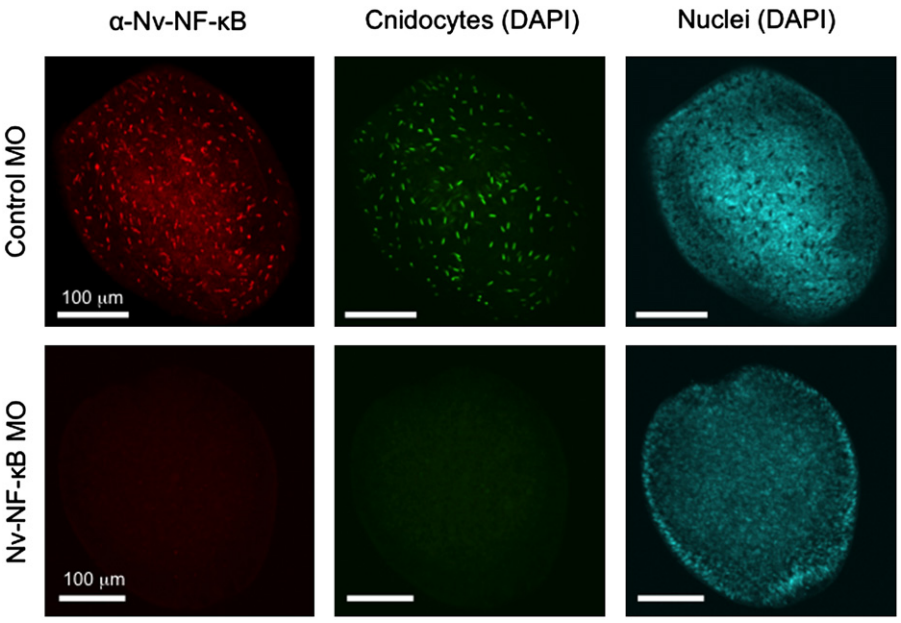

Fig. 5. Injection of Nv-NF-κB morpholinos results in a loss of cnidocyte development. Fertilized but undivided *N. vectensis* eggs were microinjected with morpholinos (MO) against a control or Nv-NF-κB transcript. Anemones were fixed under calcium-free conditions, whole-mount immunofluorescence was performed with anti-Nv-NF-κB antiserum, and antigen retrieval was not performed. Injection of the control morpholino resulted in 7 of 94 anemones that did not stain for either Nv-NF-κB or for cnidocytes (top panels). Injection of the Nv-NF-κB morpholino resulted in 60 of 66 anemones that did not stain for either NF-κB or cnidocytes (bottom panels). By a Fisher's Exact Test (Two-tailed) the difference in Nv-NF-κB/cnidocyte knockdown between the control and Nv-NF-κB morpholino groups is statistically significant ($P < 0.0001$).

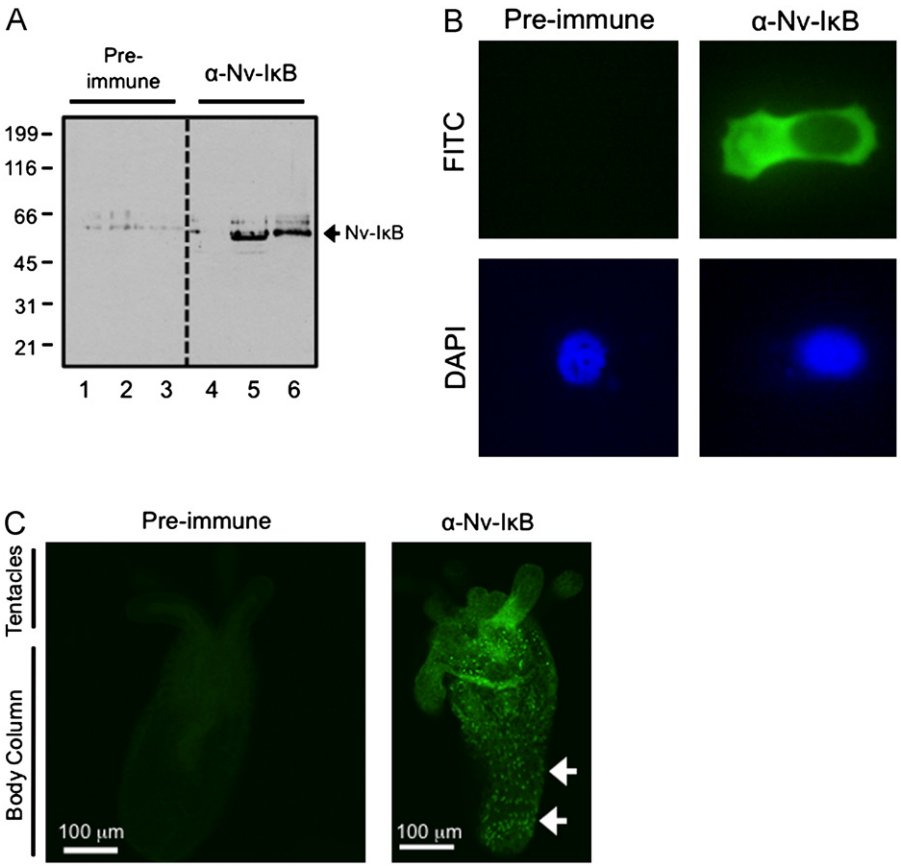

Fig. 6. Nv-IκB is expressed in a subset of ectodermal cells in *N. vectensis*. (A) Anti-Nv-IκB Western blotting of A293 cells transfected with empty vector (lanes 1 and 4), pcDNA-Nv-IκB (lanes 2 and 5), or of an extract from an adult *Nematostella* (lanes 3 and 6). The membrane was probed with either pre-immune serum (lanes 1–3) or anti-Nv-IκB antiserum (lanes 4–6). A dotted line indicates where the membrane was cut prior to Western blotting. Nv-IκB is indicated by the arrow, and molecular mass markers (in kDa) are indicated to the left of the figure. (B) DF-1 chicken fibroblast cells were transfected with pcDNA-Nv-IκB. Indirect immunofluorescence was then performed using either pre-immune serum or anti-Nv-IκB antiserum, which was detected with FITC-conjugated secondary antiserum (upper panels). Nuclei were stained with DAPI (lower panel). (C) Whole-mount immunofluorescence was performed on polyps with pre-immune serum (left) or anti-Nv-IκB antiserum (right) and detected with FITC-conjugated secondary antiserum. Arrows indicate regions with specifically stained individual cells. Antigen retrieval was performed with urea. White bars indicate scale.

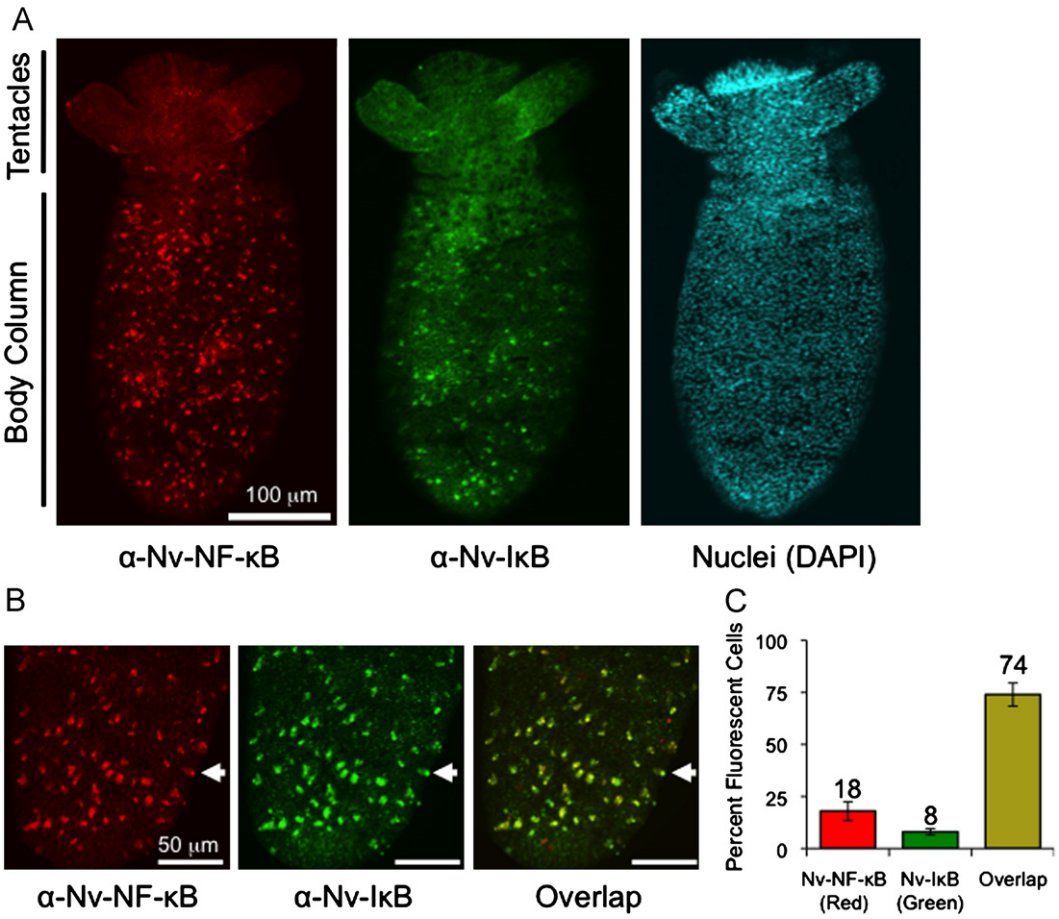

Fig. 7. Nv-NF-κB and Nv-IκB have overlapping expression in a subset of ectodermal cells. Whole-mount immunofluorescence was performed with anti-Nv-NF-κB and anti-Nv-IκB antisera and antigen retrieval was performed with urea. (A) Nv-NF-κB staining was detected with Texas Red (left panels), Nv-IκB staining with FITC (middle panels), and nuclei with DAPI (right panels). (B) An overlapped image of a whole-mount juvenile polyp shows Nv-NF-κB (left), Nv-IκB (middle) and overlapping staining (right). Arrows indicate overlapping stain. White bars indicate scale. (C) A total of 693 fluorescent cells were counted in five anemones and sorted based on staining for Texas Red (Nv-NF-κB), FITC (Nv-IκB) or both. Values correspond to the percentage of total fluorescent cells. Error bars indicate standard error. (For interpretation of the references to color in this figure legend, the reader is referred to the web version of this article.)

anti-Nv-NF-κB staining (Nv-IκB, Fig. 6C; Nv-NF-κB, Fig. 1A). To determine whether individual cells express both proteins, indirect immunofluorescence was performed with antisera against both Nv-NF-κB and Nv-IκB. In whole-mount staining of polyps, both proteins were primarily detected in body column cells and were absent from oral tissues and tentacles (Fig. 7A, black bars). In a merged image, Nv-NF-κB and Nv-IκB staining largely overlapped in the body column of a juvenile polyp (Fig. 7B). Quantification of immune-reactive cells over five anemones showed that 74% of cells stained positive for both Nv-NF-κB and Nv-IκB (Fig. 7C; right column). By comparison, 18% of the cells stained positive for Nv-NF-κB only and 8% were positive for Nv-IκB only. The overlapping expression of Nv-NF-κB and IκB combined with the overlapping expression of Nv-NF-κB with a cnidocyte stain indicate that Nv-IκB is expressed in this subset of cnidocytes as well.

Discussion

The results in this paper indicate that NF-κB is required for the development of cnidocytes in the body column of *N. vectensis*. That is, Nv-NF-κB is expressed in cnidocytes of juvenile and adult animals, is located in the nucleus of a subset of cells in the 30-h post-fertilization embryo, and morpholino-mediated knockdown of Nv-NF-κB expression results in a dramatic reduction in cnidocyte staining in later animals. Taken together, these results are consistent with the hypothesis that nuclear Nv-NF-κB in the 30-h embryo controls the expression of genes that specify the development of cnidocytes in the anemone. The distribution of the Nv-NF-κB-positive cnidocytes in the body column and their size indicate that they are part of the BH subtype of cnidocytes. The function of BH cnidocytes in *N. vectensis* is not well understood (Zenkert et al., 2011).

Not all body column cnidocytes co-stained for Nv-NF-κB and DAPI (Fig. 1E). We offer two explanations for the 22% of cells that stained positive for Nv-NF-κB only: (1) these cells may be immature cnidocytes and lack sufficient poly-γ-glutamate to be stained by DAPI; and (2) the lack of double staining may be a technical issue because DAPI staining of poly-γ-glutamate is transient and diffuses overnight. Of the remaining body column cnidocytes that stained positive with DAPI but were negative for Nv-NF-κB, many are likely of the MM cnidocyte subtype, which has been reported to comprise 5–22% of total cnidocytes depending on the developmental stage (Zenkert et al., 2011).

In juvenile anemones, Nv-NF-κB is located in the cytoplasm of a subset of cnidocytes in the body column of the animal. The co-expression of Nv-NF-κB and Nv-IκB in this same subset of cells (Fig. 7C), as well as the ability of Nv-IκB to retain Nv-NF-κB in the cytoplasm when expressed in vertebrate cells (Wolenski et al., 2011b), suggest that Nv-IκB is responsible for the cytoplasmic

localization of Nv-NF-κB in the body column cells. Unfortunately, we have not yet been able to identify a treatment that can induce nuclear localization of Nv-NF-κB and degradation of Nv-IκB in adult animals. Thus, it is not clear whether there is a condition or stimulus that can induce nuclear activation of Nv-NF-κB in cnidocytes in mature animals.

In contrast to adult animals, Nv-NF-κB is constitutively nuclear in the 30-h embryo. Whether a signal induces nuclear localization of Nv-NF-κB in early embryonic cells (e.g., at 30 h post-fertilization) is not known. *N. vectensis* does, however, have genes that appear to encode Toll-like receptors (Miller et al., 2007; Sullivan et al., 2007), which are required for nuclear localization of Dorsal in the *Drosophila* embryo (Ganesan et al., 2011). Alternatively, Nv-NF-κB may be nuclear in the early embryo due to a lack of Nv-IκB expression. Indeed, in early stages of development, we have not been able to detect Nv-IκB-positive cells, even at time points (e.g., 30 h post-fertilization) when Nv-NF-κB is expressed (data not shown). However, we cannot exclude that Nv-IκB is not detected because the reactivity of the anti-Nv-IκB antiserum is too weak. Whether the nuclear Nv-NF-κB is expressed in cells that later develop into mature cnidocytes or the Nv-NF-κB-positive cells have an indirect effect on cnidocyte development is not clear from our experiments.

Recently, Notch signaling was shown to be critical for the development of both cnidocytes and neurons in *N. vectensis*, suggesting that the two cell types share a common origin as multifunctional sensory-effecter cells (Marlow et al., 2012). Treatment of fertilized *N. vectensis* eggs with the γ-secretase inhibitor DAPT, which is an inhibitor of Notch activation, results in a decrease in the number of cnidocytes in 3 day-old animals (Marlow et al., 2012). In our hands, treatment of fertilized *Nematostella* eggs with DAPT prevented the later development of cnidocytes and Nv-NF-κB expression was also not detected (Supplemental Fig. 4). Thus, a Notch-to-NF-κB pathway appears to control cnidocyte development in *Nematostella.* Of note, in some vertebrate cells, DAPT can inhibit both Notch processing (Geling et al., 2002) and its ability to activate downstream NF-κB signaling (Monsalve et al., 2009).

Our results indicate that Nv-NF-κB contributes to cnidocyte development in anemones. The involvement of Nv-NF-κB in a developmental program is reminiscent of the role that the NF-κB-like protein Dorsal plays in dorsal-ventral embryonic polarity in *Drosophila*, a biological function for NF-κB that appears to be insect-specific. However, NF-κB signaling also plays a role in several other biological processes in *Drosophila* (Gilmore and Wolenski, 2012). Thus, Nv-NF-κB may have additional biological roles in anemones. Nevertheless, it is apparent that the role of NF-κB in cnidocyte development in anemones is an evolutionarily derived one, given that other basal animals (e.g., sponges) that have NF-κB do not have cnidoctyes.

Acknowledgments

We thank Finnegan Hewitt and Mandy Core for assistance with morpholino injections, Eric Röttinger for help in morpholino design, Derek Stefanik for help with animal maintenance and spawning, and Todd Blute, Jan Blom, and Jeannette Connerney for help with immunohistochemistry and microscopy. This research was supported by National Science Foundation grant MCB-0924749 (J.R.F., T.D.G.). F.S.W. was supported by a predoctoral grant from the Superfund Basic Research Program at Boston University (5 P42 ES07381) and a Warren-McLeod Graduate Fellowship in Marine Biology.

Appendix A. Supporting information

Supplementary data associated with this article can be found in the online version at http://dx.doi.org/10.1016/j.ydbio.2012.10.004.

References

Augustin, R., Fraune, S., Bosch, T.C., 2010. How *Hydra* senses and destroys microbes. Semin. Immunol. 22, 54–58.
Beg, A.A., Sha, W.C., Bronson, R.T., Ghosh, S., Baltimore, D., 1995. Embryonic lethality and liver degeneration in mice lacking the RelA component of NF-κB. Nature 376, 167–170.
Burgess, A., Vigneron, S., Brioudes, E., Labbé, J.C., Lorca, T., Castro, A., 2010. Loss of human Greatwall results in G2 arrest and multiple mitotic defects due to deregulation of the cyclin B-Cdc2/PP2A balance. Proc. Natl. Acad. Sci. U.S.A. 107, 12564–12569.
Bushdid, P.B., Brantley, D.M., Yull, F.E., Blaeuer, G.L., Hoffman, L.H., Niswander, L., Kerr, L.D., 1998. Inhibition of NF-κB activity results in disruption of the apical ectodermal ridge and aberrant limb morphogenesis. Nature 392, 615–618.
Darling, J.A., Reitzel, A.R., Burton, P.M., Mazza, M.E., Ryan, J.F., Sullivan, J.C., Finnerty, J.R., 2005. Rising starlet: the starlet sea anemone, *Nematostella vectensis*. BioEssays 27, 211–221.
Fritzenwanker, J.H., Technau, U., 2002. Induction of gametogenesis in the basal cnidarian *Nematostella vectensis* (Anthozoa). Dev. Genes Evol. 212, 99–103.
Ganesan, S., Aggarwal, K., Paquette, N., Silverman, N., 2011. NF-κB/Rel proteins and the humoral immune responses of *Drosophila melanogaster*. Curr. Top. Microbiol. Immunol. 349, 25–60.
Gauthier, M., Degnan, B.M., 2008. The transcription factor NF-κB in the demosponge *Amphimedon queenslandica*: insights on the evolutionary origin of the Rel homology domain. Dev. Genes Evol. 218, 23–32.
Geling, A., Steiner, H., Willem, M., Bally-Cuif, L., Haass, C., 2002. A γ-secretase inhibitor blocks Notch signaling in vivo and causes a severe neurogenic phenotype in zebrafish. EMBO Rep. 3, 688–694.
Genikhovich, G., Technau, U., 2009. Induction of spawning in the starlet sea anemone Nematostella vectensis, in vitro fertilization of gametes, and dejellying of zygotes. Cold Spring Harbor Protoc. 2009, pdb prot5281.
Gerondakis, S., Grumont, R., Gugasyan, R., Wong, L., Isomura, I., Ho, W., Banerjee, A., 2006. Unravelling the complexities of the NF-κB signalling pathway using mouse knockout and transgenic models. Oncogene 25, 6781–6799.
Gilmore, T.D., Wolenski, F.S., 2012. NF-κB: where did it come from and why? Immunol. Rev. 246, 14–35.
Hand, C., Uhlinger, K.R., 1994. The unique, widely distributed, estuarine sea anemone, *Nematostella vectensis* Stephenson: a review, new facts, and questions. Estuaries 17, 501–508.
Hayden, M.S., Ghosh, S., 2004. Signaling to NF-κB. Genes Dev. 18, 2195–2224.
Hayden, M.S., Ghosh, S., 2008. Shared principles in NF-κB signaling. Cell 132, 344–362.
Kanegae, Y., Tavares, A.T., Izpisua Belmonte, J.C., Verma, I.M., 1998. Role of Rel/NF-κB transcription factors during the outgrowth of the vertebrate limb. Nature 392, 611–614.
Kass-Simon, G., Scappaticci, J.A.A., 2002. The behavioral and developmental physiology of nematocysts. Can. J. Zool. 80, 1772–1794.
Krayesky, S., Mahoney, J., Kinler, K., Peltier, S., Calais, W., Allaire, K., Watson, G., 2010. Regulation of spirocyst discharge in the model sea anemone, *Nematostella vectensis*. Mar. Biol. 157, 1041–1047.
Lange, C., Hemmrich, G., Klostermeier, U.C., López-Quintero, J.A., Miller, D.J., Rahn, T., Weiss, Y., Bosch, T.C., Rosenstiel, P., 2011. Defining the origins of the NOD-like receptor system at the base of animal evolution. Mol. Biol. Evol. 28, 1687–1702.
Layden, M.J., Meyer, N.P., Pang, K., Seaver, E.C., Martindale, M.Q., 2010. Expression and phylogenetic analysis of the *zic* gene family in the evolution and development of metazoans. EvoDevo 1, 12.
Lynch, J.A., Roth, S., 2011. The evolution of dorsal-ventral patterning mechanisms in insects. Genes Dev. 25, 107–118.
Mariscal, R.N., McLean, R.B., Hand, C., 1977. The form and function of cnidarian spirocysts. 3. Ultrastructure of the thread and the function of spirocysts. Cell Tissue Res. 178, 427–433.
Marlow, H., Roettinger, E., Boekhout, M., Martindale, M.Q., 2012. Functional roles of Notch signaling in the cnidarian *Nematostella vectensis*. Dev. Biol. 362, 295–308.
Marlow, H.Q., Srivastava, M., Matus, D.Q., Rokhsar, D., Martindale, M.Q., 2009. Anatomy and development of the nervous system of *Nematostella vectensis*, an anthozoan cnidarian. Dev. Neurobiol. 69, 235–254.
Meyer, E., Aglyamova, G.V., Wang, S., Buchanan-Carter, J., Abrego, D., Colbourne, J.K., Willis, B.L., Matz, M.V., 2009. Sequencing and *de novo* analysis of a coral larval transcriptome using 454 GSFlx. BMC Genomics 10, 219.
Miller, D.J., Hemmrich, G., Ball, E.E., Hayward, D.C., Khalturin, K., Funayama, N., Agata, K., Bosch, T.C., 2007. The innate immune repertoire in Cnidaria—ancestral complexity and stochastic gene loss. Genome Biol. 8, R59.
Monsalve, E., Ruiz-García, A., Baladrón, V., Ruiz-Hidalgo, M.J., Sánchez-Solana, B., Rivero, S., Garcia-Ramírez, J.J., Rubio, A., Laborda, J., Diaz-Guerra, M.J., 2009. Notch1 upregulates LPS-induced macrophage activation by increasing NF-κB activity. Eur. J. Immunol. 39, 2556–2570.
Oeckinghaus, A., Hayden, M.S., Ghosh, S., 2011. Crosstalk in NF-κB signaling pathways. Nat. Immunol. 12, 695–708.
Putnam, N.H., Srivastava, M., Hellsten, U., Dirks, B., Chapman, J., Salamov, A., Terry, A., Shapiro, H., Lindquist, E., Kapitonov, V.V., Jurka, J., Genikhovich, G., Grigoriev, I.V., Lucas, S.M., Steele, R.E., Finnerty, J.R., Technau, U., Martindale, M.Q., Rokhsar, D.S., 2007. Sea anemone genome reveals ancestral eumetazoan gene repertoire and genomic organization. Science 317, 86–94.

Reitzel, A., Darling, J., Sullivan, J., Finnerty, J., 2008. Global population genetic structure of the starlet anemone *Nematostella vectensis*: multiple introductions and implications for conservation policy. Biol. Invas. 10, 1197–1213.

Sebé-Pedrós, A., de Mendoza, A., Lang, B.F., Degnan, B.M., Ruiz-Trillo, I., 2011. Unexpected repertoire of metazoan transcription factors in the unicellular holozoan *Capsaspora owczarzaki*. Mol. Biol. Evol. 28, 1241–1254.

Shi, S.R., Chaiwun, B., Young, L., Cote, R.J., Taylor, C.R., 1993. Antigen retrieval technique utilizing citrate buffer or urea solution for immunohistochemical demonstration of androgen receptor in formalin-fixed paraffin sections. J. Histochem. Cytochem. 41, 1599–1604.

Shinzato, C., Shoguchi, E., Kawashima, T., Hamada, M., Hisata, K., Tanaka, M., Fujie, M., Fujiwara, M., Koyanagi, R., Ikuta, T., Fujiyama, A., Miller, D.J., Satoh, N., 2011. Using the *Acropora digitifera* genome to understand coral responses to environmental change. Nature 476, 320–323.

Steele, R.E., David, C.N., Technau, U., 2011. A genomic view of 500 million years of cnidarian evolution. Trends Genet. 27, 7–13.

Stephenson, T.A., 1935. The British Sea Anemones, Volume II. Ray Society, London.

Sullivan, J.C., Kalaitzidis, D., Gilmore, T.D., Finnerty, J.R., 2007. Rel homology domain-containing transcription factors in the cnidarian *Nematostella vectensis*. Dev. Genes Evol. 217, 63–72.

Sullivan, J.C., Ryan, J.F., Watson, J.A., Webb, J., Mullikin, J.C., Rokhsar, D., Finnerty, J.R., 2006. StellaBase: the *Nematostella vectensis* genomics database. Nucleic Acids Res. 34, D495–D499.

Sullivan, J.C., Wolenski, F.S., Reitzel, A.M., French, C.E., Traylor-Knowles, N., Gilmore, T.D., Finnerty, J.R., 2009. Two alleles of NF-κB in the sea anemone *Nematostella vectensis* are widely dispersed in nature and encode proteins with distinct activities. PLoS ONE 4, e7311.

Szczepanek, S., Cikala, M., David, C.N., 2002. Poly-γ-glutamate synthesis during formation of nematocyst capsules in *Hydra*. J. Cell Sci. 115, 745–751.

Watson, G., Mire, P., Kinler, K., 2009. Mechanosensitivity in the model sea anemone *Nematostella vectensis*. Mar. Biol. 156, 2129–2137.

Watson, G.M., Mariscal, R.N., 1983. Comparative ultrastructure of catch tentacles and feeding tentacles in the sea anemone *Haliplanella*. Tissue Cell 15, 939–953.

Weis, V.M., 2008. Cellular mechanisms of Cnidarian bleaching: stress causes the collapse of symbiosis. J. Exp. Biol. 211, 3059–3066.

Wolenski, F.S., Chandani, S., Stefanik, D.J., Jiang, N., Chu, E., Finnerty, J.R., Gilmore, T.D., 2011a. Two polymorphic residues account for the differences in DNA binding and transcriptional activation by NF-κB proteins encoded by naturally occurring alleles in *Nematostella vectensis*. J. Mol. Evol. 73, 325–336.

Wolenski, F.S., Garbati, M.R., Lubinski, T.J., Traylor-Knowles, N., Dresselhaus, E., Stefanik, D.J., Goucher, H., Finnerty, J.R., Gilmore, T.D., 2011b. Characterization of the core elements of the NF-κB signaling pathway of the sea anemone *Nematostella vectensis*. Mol. Cell. Biol. 31, 1076–1087.

Zenkert, C., Takahashi, T., Diesner, M.O., Özbek, S., 2011. Morphological and molecular analysis of the *Nematostella vectensis* cnidom. PLoS ONE 6, e22725.